

Effects of geometrical nonlinearities on the acoustic black hole effect

Vivien Denis^{1,3}, Adrien Pelat¹, Cyril Touzé², François Gautier¹
vivien.denis@ensam.eu

¹Laboratoire d'Acoustique de l'Université du Maine, Le Mans, France
UMR CNRS 6613

²Laboratoire des Sciences de l'Information et des Systèmes, Lille, France
UMR CNRS 7296

³IMSIA, ENSTA Paritech, Palaiseau, France
UMR EDF-ENSTA-CNRS-CEA 9219

GDR Dynolin 2016, 11 octobre 2016

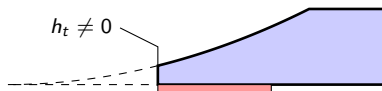


Introduction : Acoustic Black Hole (ABH)

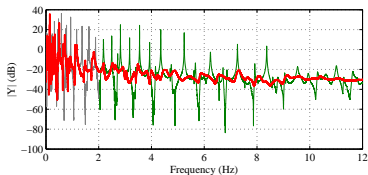
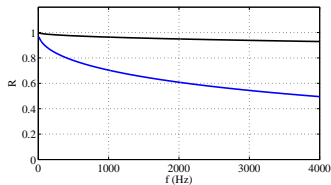
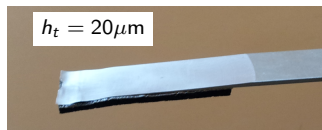
Acoustic Black Hole effet

- ▶ Thin structure, flexural waves
- ▶ Viscoelastic layer
- ▶ $\text{Im}(k_f) \nearrow \Rightarrow R \searrow$
- ▶ Damping without adding mass

[Mironov, 1988], [Krylov et al., 2004]



$$h(x) = \epsilon x^m, m \geq 2 \Rightarrow \lambda, c \xrightarrow{x \rightarrow 0} 0$$

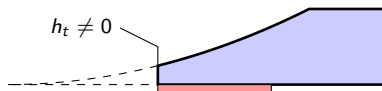


Introduction : Acoustic Black Hole (ABH)

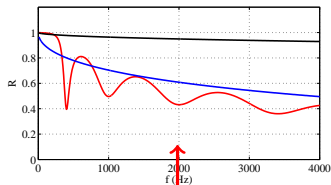
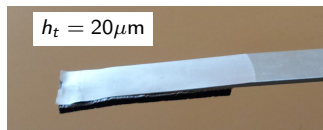
Acoustic Black Hole effet

- ▶ Thin structure, flexural waves
- ▶ Viscoelastic layer
- ▶ $\text{Im}(k_f) \nearrow \Rightarrow R \searrow$
- ▶ Damping without adding mass

[Mironov, 1988], [Krylov et al., 2004]

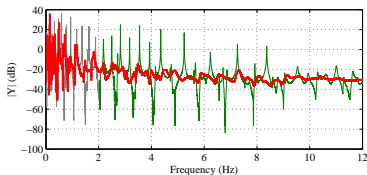


$$h(x) = \epsilon x^m, m \geq 2 \Rightarrow \lambda, c \xrightarrow{x \rightarrow 0} 0$$

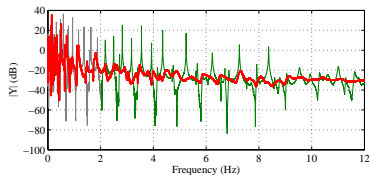


Features

- ▶ Complex variations of R [Georgiev et al., 2011]
- ▶ Smoothing of FRF \Rightarrow MOF \nearrow [Denis et al., 2014]



Introduction : Acoustic Black Hole (ABH)

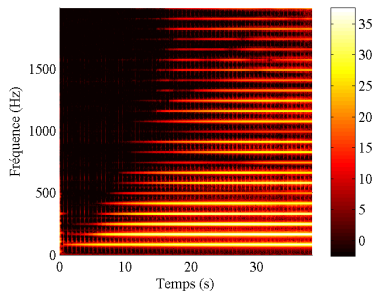
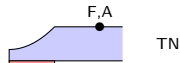
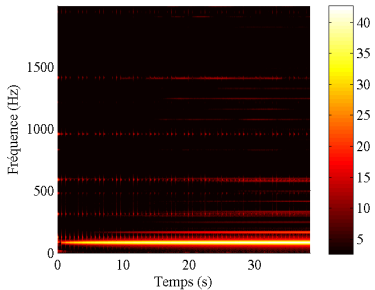
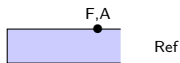


Context

- ▶ ABH inefficient at Low Frequency
- ▶ How to increase efficiency in LF?
- ▶ Large amplitude at the extremity
- ▶ Use of nonlinearities for energy transfer?

Experiment

Sine excitation $f_0=83$ Hz, increasing amplitude 0-15 N

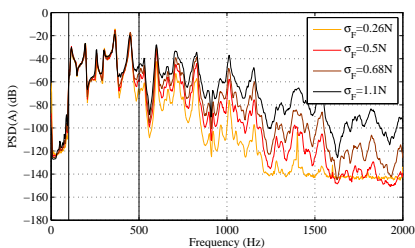
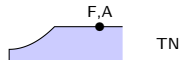
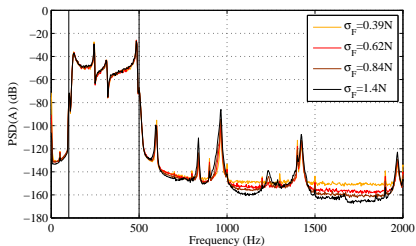
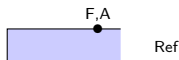


- ▶ Uniform beam is linear
- ▶ ABH beam is nonlinear
- ▶ Spectrum enrichment with amplitude (odd and even harmonics)



Experiment

Filtered white noise excitation 100-500 Hz.



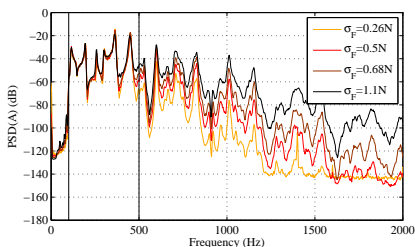
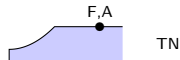
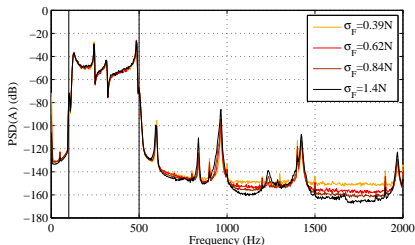
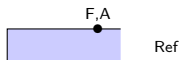
- ▶ Uniform beam : no energy leaks
- ▶ ABH beam : energy leaks \Rightarrow HF
- ▶ Transfer not sufficient for resonance peaks reduction

Dimensions 1500x20x5 mm
 $L_{abh}=300$ mm, $h_t=20$ μ m



Experiment

Filtered white noise excitation 100-500 Hz.

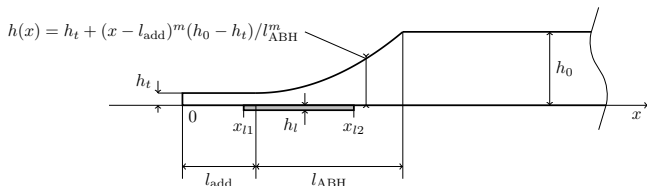


- ▶ Uniform beam : no energy leaks
- ▶ ABH beam : energy leaks \Rightarrow HF
- ▶ Transfer not sufficient for resonance peaks reduction

Conclusions

- ▶ ABH : potential for energy transfer LF \Rightarrow HF thanks to nonlinear effects
- ▶ Necessity of a model for understanding and use this effect

Model of nonlinear ABH : Development (1)



Thin Von Kármán plate, variable thickness

$$\rho h(\mathbf{x}) \ddot{w} + \Delta(D(\mathbf{x}) \Delta w) - (1 - \nu) L(D(\mathbf{x}), w) = p + L(w, F)$$

$$\Delta(A(\mathbf{x}) \Delta F) - (1 + \nu) L(A(\mathbf{x}), F) = -\frac{1}{2} L(w, w)$$

+ free boundary conditions.

$w(\mathbf{x}, t)$ transverse displacement, $F(\mathbf{x}, t)$ Airy stress function, $L(f, g) = f_{xx} g_{yy} + f_{yy} g_{xx} - 2f_{xy} g_{xy}$

[Efstathiades, 1971], [Thomas et al., 2008]

$$D(\mathbf{x}) = \frac{Eh(\mathbf{x})^3}{12(1 - \nu^2)}$$

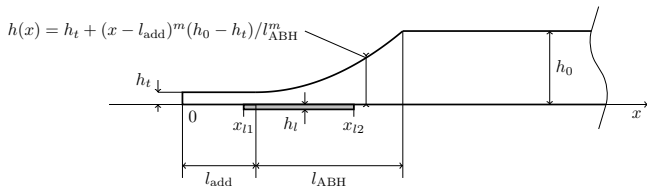
$$A(\mathbf{x}) = 1/Eh(\mathbf{x})$$

Damping

Complex bending stiffness, Ross-Ungar-Kerwin model

$$D^*(\mathbf{x}) = D(\mathbf{x})(1 + j\eta(\mathbf{x}))$$

Model of nonlinear ABH : Development (1)



Thin Von Kármán plate, variable thickness

$$\rho h \ddot{w} + \square(D, w) = p + L(w, F)$$

$$\diamond(A, F) = -L(w, w)/2$$

+ free boundary conditions.

$w(\mathbf{x}, t)$ transverse displacement, $F(\mathbf{x}, t)$ Airy stress function, $L(f, g) = f_{xx}g_{yy} + f_{yy}g_{xx} - 2f_{xy}g_{xy}$

[Efstathiades, 1971], [Thomas et al., 2008]

$$\square(D, w) = \Delta(D(\mathbf{x})\Delta w) - (1 - \nu)L(D(\mathbf{x}), w),$$

$$\diamond(A, F) = \Delta(A(\mathbf{x})\Delta F) - (1 + \nu)L(A(\mathbf{x}), F).$$

Damping

Complex bending stiffness, Ross-Ungar-Kerwin model

$$D^*(x) = D(x)(1 + j\eta(x))$$

Model of nonlinear ABH : Development (2)

Linear modes

$$-\rho h \omega^2 w + \square(D, w) = 0 \quad \Rightarrow \quad (\Phi_k, \omega_k)$$

$$\diamond(A, F) = \zeta^4 F \quad \Rightarrow \quad (\Psi_n, \zeta_n)$$

$$w = S_w \sum_{k=1}^{N_\Phi} q_k(t) \Phi_k(\mathbf{x})$$

$$F = S_F \sum_{n=1}^{N_\Psi} \beta_n(t) \Psi_n(\mathbf{x})$$

Projection on the linear modes

Quadratic formulation

$$\beta_p(t) = -\frac{S_w^2}{2\zeta_p^4 S_F} \sum_{i=1}^{N_\Phi} \sum_{j=1}^{N_\Phi} H_{i,j}^p q_i(t) q_j(t),$$

$$\ddot{q}_s(t) + \omega_s^2 q_s(t) = F_s(t) + \frac{S_F}{M_s} \sum_{k=1}^{N_\Phi} \sum_{n=1}^{N_\Psi} E_{k,n}^s q_k(t) \eta_n(t),$$

with

$$H_{i,j}^p = \int_S \Psi_p L(\Phi_i, \Phi_j) dS \quad \text{et} \quad E_{k,l}^s = \int_S L(\Phi_k, \Psi_l) \Phi_s dS.$$

⇒ can be solved with a stable numerical scheme

Model of nonlinear ABH : Development (2)

Linear modes

$$-\rho h \omega^2 w + \square(D, w) = 0 \quad \Rightarrow \quad (\Phi_k, \omega_k)$$

$$\diamond(A, F) = \zeta^4 F \quad \Rightarrow \quad (\Psi_n, \zeta_n)$$

$$w = S_w \sum_{k=1}^{N_\Phi} q_k(t) \Phi_k(\mathbf{x})$$

$$F = S_F \sum_{n=1}^{N_\Psi} \beta_n(t) \Psi_n(\mathbf{x})$$

Projection on the linear modes

Cubic formulation

$$\ddot{q}_s(t) + \omega_s^2 q_s(t) = F_s(t) - \frac{S_w^2}{M_s} \sum_{k=1}^{N_\Phi} \sum_{m=1}^{N_\Phi} \sum_{n=1}^{N_\Phi} \Gamma_{k,m,n}^s q_k(t) q_m(t) q_n(t)$$

avec

$$\Gamma_{k,m,n}^s = \sum_{l=1}^{N_\Psi} \frac{H_{m,n}^l E_{k,l}^s}{2\zeta_l^4}.$$

⇒ useful for evaluating the convergence

Model of nonlinear ABH : Development (2)

Linear modes

$$-\rho h \omega^2 w + \square(D, w) = 0 \Rightarrow (\Phi_k, \omega_k)$$

$$\diamond(A, F) = \zeta^4 F \Rightarrow (\Psi_n, \zeta_n)$$

Dissipative problem

$$-\rho h \omega^2 w + \square(D^*, w) = 0$$

$$\Rightarrow (\Phi_k^*, \omega_k^*) \Rightarrow \xi_k$$

Projection on the linear modes

Quadratic formulation with dissipation

$$\beta_p(t) = -\frac{S_w^2}{2\zeta_p^4 S_F} \sum_{i=1}^{N_\Phi} \sum_{j=1}^{N_\Phi} H_{i,j}^p q_i(t) q_j(t),$$

$$\ddot{q}_s(t) + 2\xi_s \omega_s \dot{q}_s(t) + \omega_s^2 q_s(t) = F_s(t) + \frac{S_F}{M_s} \sum_{k=1}^{N_\Phi} \sum_{n=1}^{N_\Psi} E_{k,n}^s q_k(t) \eta_n(t),$$

\Rightarrow can be solved with a stable numerical scheme

Model of nonlinear ABH : Numerical resolution, modes

Finite difference method

Grid adapted to wavelength variation

$$d\tilde{x} = \frac{1}{\sqrt{h(x)}} dx$$

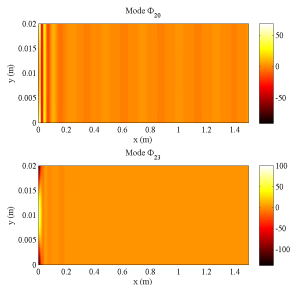


Discrete problem

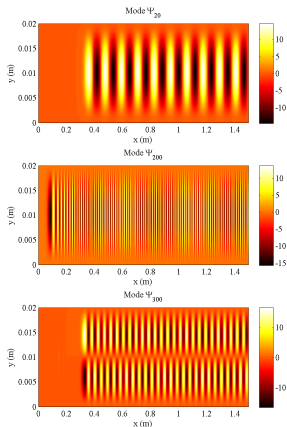
$$(\mathbf{K} - \alpha^2 \mathbf{M}) \mathbf{W} = 0$$

[Denis et al., 2014]

Transverse modes Φ



In-plane modes Ψ



$\Rightarrow \Psi$ modes are sorted by families N ($N + 1$ nodal lines along y)

Model of nonlinear ABH : Numerical resolution, integration

Conservative scheme

$$\delta_{tt} q_s(n) + 2\xi_s \omega_s \delta_t q_s(n) + \omega_s^2 q_s(n) = \frac{S_F}{M_s} \sum_{k=1}^{N_\Phi} \sum_{l=1}^{N_\Psi} E_{k,l}^s q_k(n) [\mu_t \cdot \eta_l(n)] + F_s(n)$$
$$\mu_{t-\beta_p}(n) = \frac{-S_w^2}{2\zeta_p^4 S_F} \sum_{i=1}^{N_\Phi} \sum_{j=1}^{N_\Phi} H_{i,j}^p q_i [e_t - q_j(n)]$$

[Ducceschi et al., 2015]

Finite difference operators

$$\delta_{t+w_n} = \frac{w_{n+1} - w_n}{\Delta t},$$
$$\delta_{tt} = \frac{w_{n+1} - 2w_n + w_{n-1}}{\Delta t^2},$$
$$\mu_{t+w_n} = \frac{w_{n+1} + w_n}{2}.$$

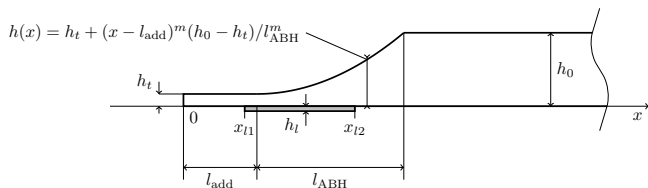
Stability condition

$$f_e > \pi f_{max}$$

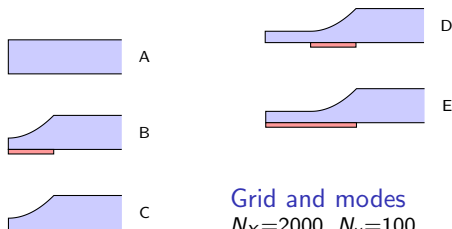
$f_e = 1/\Delta t$ sampling rate

f_{max} frequency of highest mode

Simulated beams



Geometry	
L	1.5 m
b	20 mm
h_0	5 mm
h_t	50 μm
l_{ABH}	30 cm
l_{add}	0 ou 10 cm
h_l	100 μm
Material	
E	70 GPa
ρ	2700 $\text{kg}\cdot\text{m}^{-3}$
ν	0.3
E_l	1 GPa
ρ_l	1000 $\text{kg}\cdot\text{m}^{-3}$
η_l	0.4



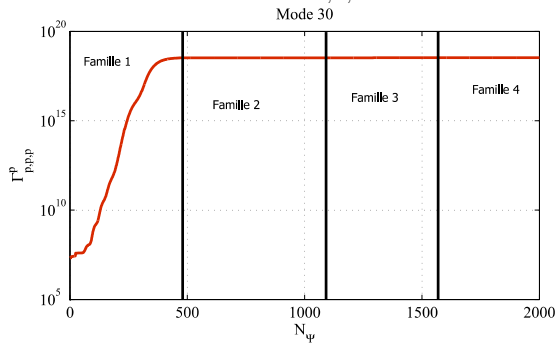
Grid and modes

$N_x=2000, N_y=100$

$N_\phi=100, N_\psi=2000$

Numerical results : Convergence

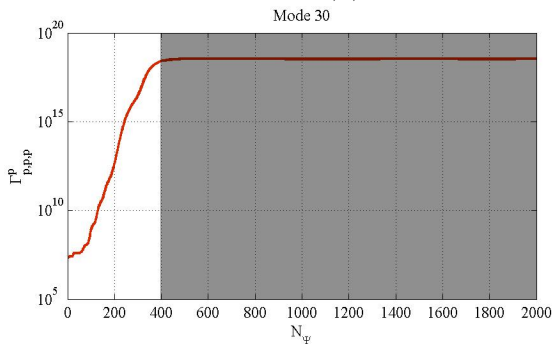
Convergence of coupling terms $\Gamma_{k,m,n}^s$ with N_Ψ



- Ψ modes sorted by families \Rightarrow Faster convergence

Numerical results : Convergence

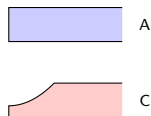
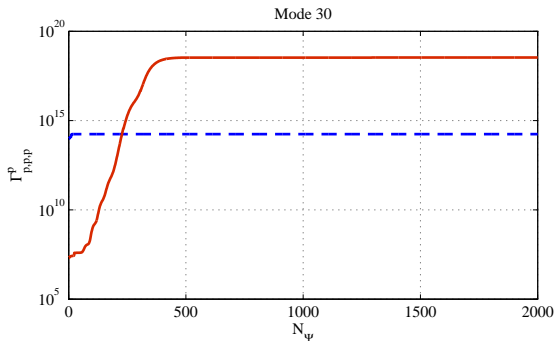
Convergence of coupling terms $\Gamma_{k,m,n}^s$ with N_Ψ



- ▶ Ψ modes sorted by families \Rightarrow Faster convergence
- ▶ Elimination of the useless modes (only family 1 contributes)

Numerical results : Convergence

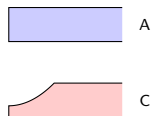
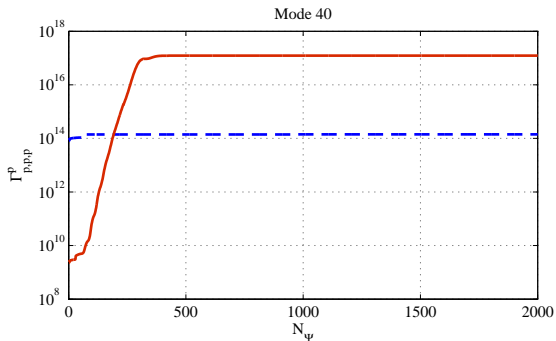
Convergence of coupling terms $\Gamma_{k,m,n}^s$ with N_Ψ



- ▶ Ψ modes sorted by families \Rightarrow Faster convergence
- ▶ Elimination of the useless modes (only family 1 contributes)
- ▶ Higher coupling coefficient for ABH beam

Numerical results : Convergence

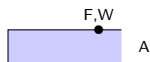
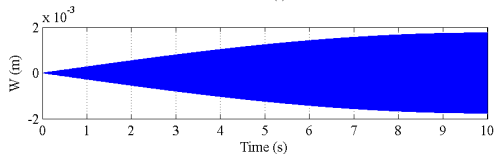
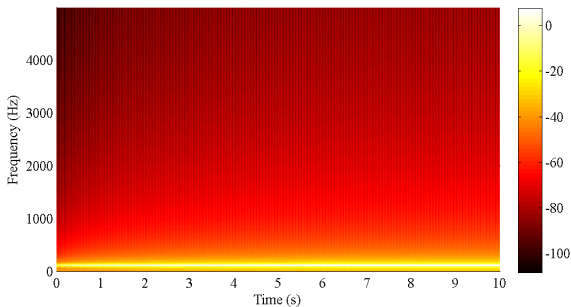
Convergence of coupling terms $\Gamma_{k,m,n}^s$ with N_Ψ



- ▶ Ψ modes sorted by families \Rightarrow Faster convergence
- ▶ Elimination of the useless modes (only family 1 contributes)
- ▶ Higher coupling coefficient for ABH beam

Numerical results : Nonlinear regimes

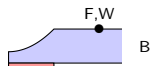
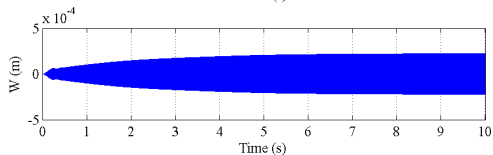
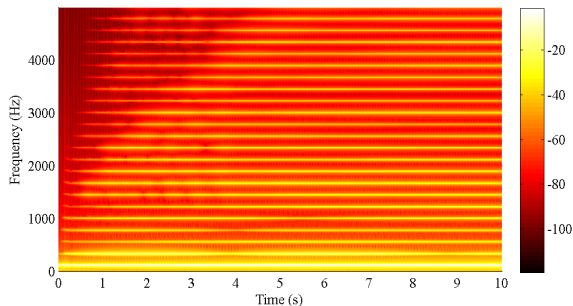
Sine excitation $f_0=111$ Hz, increasing amplitude 0-20 N, point (0.6,0.01) m, $f_e=100$ kHz



- ▶ Linear regime for uniform beam

Numerical results : Nonlinear regimes

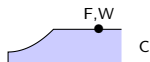
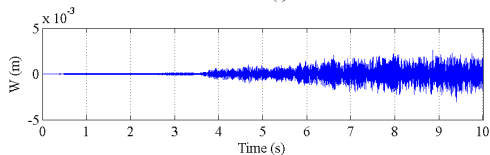
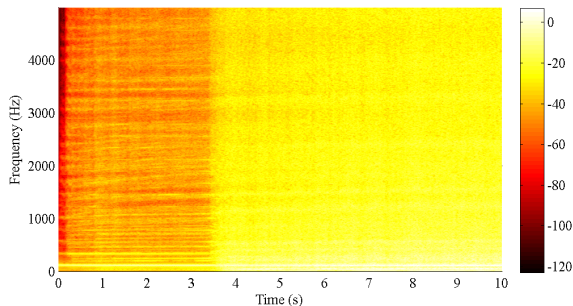
Sine excitation $f_0=111$ Hz, increasing amplitude 0-20 N, point (0.6,0.01) m, $f_e=100$ kHz



- ▶ Linear regime for uniform beam
- ▶ Rich spectrum with odd harmonics

Numerical results : Nonlinear regimes

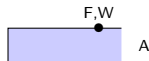
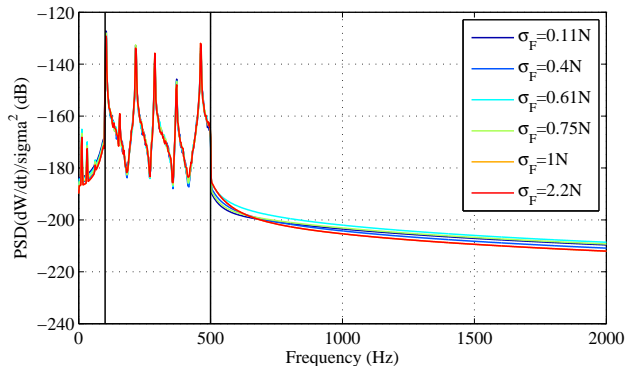
Sine excitation $f_0=111$ Hz, increasing amplitude 0-20 N, point (0.6,0.01) m, $f_e=100$ kHz



- ▶ Linear regime for uniform beam
- ▶ Rich spectrum with odd harmonics
- ▶ Chaotic regime

Numerical results : Energy transfer

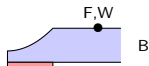
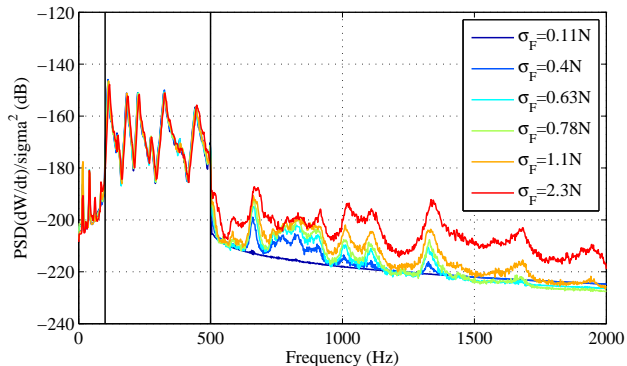
Filtered white noise excitation 100-500 Hz, point (0.6,0.01) m, $f_e=100$ kHz



- ▶ Linearity of the uniform beam

Numerical results : Energy transfer

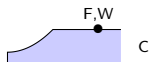
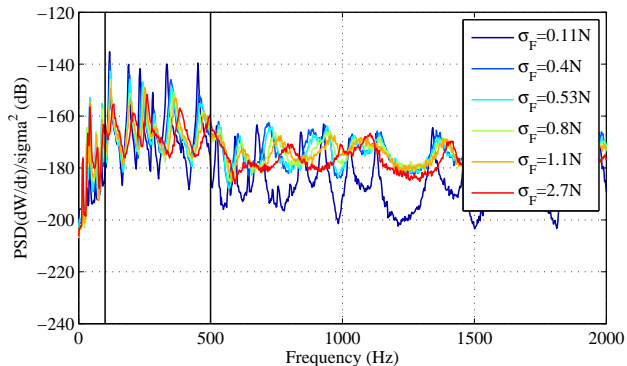
Filtered white noise excitation 100-500 Hz, point (0.6,0.01) m, $f_e=100$ kHz



- ▶ Energy leaks with amplitude increase
- ▶ Slight reduction of resonances peaks at LF with amplitude
- ▶ Increase of resonance frequencies (hardening)

Numerical results : Energy transfer

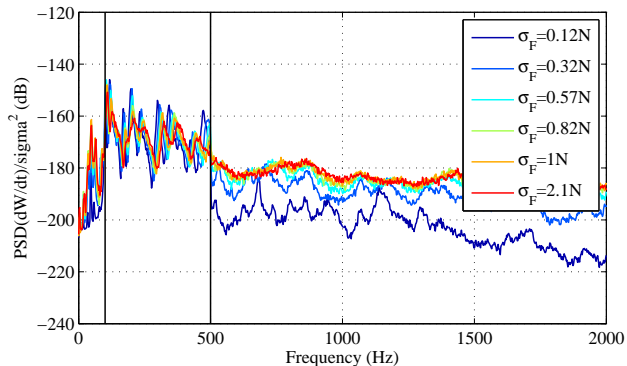
Filtered white noise excitation 100-500 Hz, point (0.6,0.01) m, $f_e=100$ kHz



- ▶ Important energy transfer \Rightarrow HF
- ▶ LF reduction even without damping

Numerical results : Energy transfer

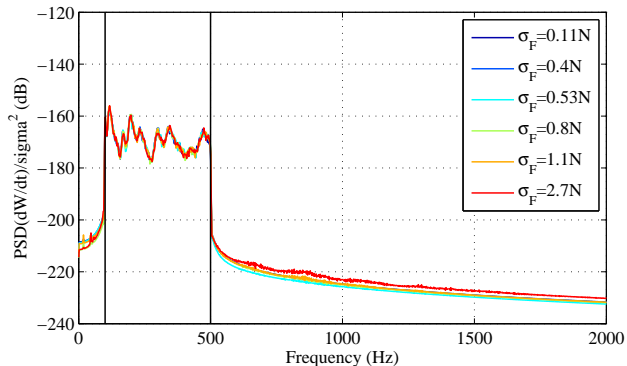
Filtered white noise excitation 100-500 Hz, point (0.6,0.01) m, $f_e=100$ kHz



- ▶ Increase nonlinear effects with the extension
- ▶ Important LF vibration reduction

Numerical results : Energy transfer

Filtered white noise excitation 100-500 Hz, point (0.6,0.01) m, $f_e=100$ kHz



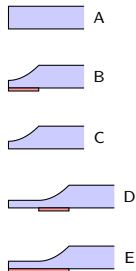
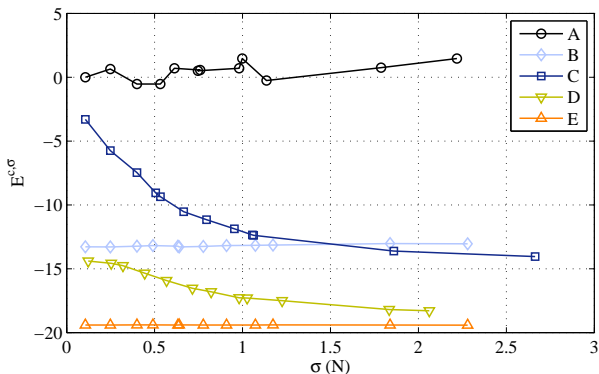
- ▶ Too much damping kills nonlinearities

Numerical results : Energy transfer

Indicator of ABH performance
in low-frequency

$$I^{c,\sigma} = \int_{100}^{500} \frac{S_{aa}^{c,\sigma}(f)}{S_{pp}^{c,\sigma}(f)} df$$

$$E^{c,\sigma} = 10 \log_{10} \left(\frac{I^{c,\sigma}}{I^{\text{ref}}} \right)$$



- ▶ Reduction of LF energy due to nonlinearity
- ▶ Damping kills nonlinear effects
- ▶ Right balance between damping and nonlinear extension has to be adjusted

Conclusions

Conclusions

- ▶ Numerical model for nonlinear ABH
- ▶ ABH profile gives nonlinear behaviour to the beam
- ▶ LF to HF energy transfer : better performance of ABH in LF
- ▶ Viscoelastic layer calms down NLs
- ▶ Extension increases nonlinear effects
- ▶ Indicator of ABH performance

Future works

- ▶ Right balance between damping and nonlinear extension has to be adjusted
- ▶ Obtain nonlinearity for small excitation amplitude
- ▶ Observe benefits experimentally

Effects of geometrical nonlinearities on the acoustic black hole effect

Vivien Denis^{1,3}, Adrien Pelat¹, Cyril Touzé², François Gautier¹
vivien.denis@ensam.eu

¹Laboratoire d'Acoustique de l'Université du Maine, Le Mans, France
UMR CNRS 6613

²Laboratoire des Sciences de l'Information et des Systèmes, Lille, France
UMR CNRS 7296

³IMSIA, ENSTA Paritech, Palaiseau, France
UMR EDF-ENSTA-CNRS-CEA 9219

GDR Dynolin 2016, 11 octobre 2016

